

# Supplementary material to: Loss of accumulation zone exposes dark ice and drives increased ablation at Weißseespitze, Austria

Lea Hartl<sup>1,2</sup>, Federico Covi<sup>3</sup>, Martin Stocker-Waldhuber<sup>1</sup>, Anna Baldo<sup>1,4</sup>, Davide Fugazza<sup>4</sup>, Biagio Di Mauro<sup>5</sup>, and Kathrin Naegeli<sup>6</sup>

<sup>1</sup>Institute for Interdisciplinary Mountain Research, Austrian Academy of Sciences, Innrain 25, 6020 Innsbruck, Austria

<sup>2</sup>Alaska Climate Research Center, University of Alaska Fairbanks, 2156 Koyukuk Drive, Fairbanks, AK 99775, USA

<sup>3</sup>British Antarctic Survey, Cambridge, United Kingdom

<sup>4</sup>Consiglio Nazionale delle Ricerche - Istituto di Scienze Polari, Milan, Italy

<sup>5</sup>Department of Environmental Science and Policy, Università degli Studi di Milano, Milan, Italy

<sup>6</sup>Department of Geography, University of Zurich, Zurich, Switzerland

**Correspondence:** L. Hartl (lea.hartl@oeaw.ac.at)

## 1 Impact of surface slope on daily albedo calculation

The glacier surface at the WSS AWS is slightly sloped in a northeasterly direction, at an angle of around 6°-8° degrees as per the 2017 DEM. The exact slope angle varies with snow cover and ice ablation and is unknown. The sensor alignment on the mast can deviate from the horizontal, especially in winter when the snow pack causes tension on the guy wires. The slope of the incident plane results in a systematic error in the measurement of reflected radiation ( $SW_{ref}$ ). On cloud free days, this is apparent in a temporal shift between the diurnal curves of incoming and reflected SW radiation such that the maximum of reflected SW radiation occurs before the maximum of incoming SW radiation (Fig. S1).

To estimate the magnitude of the potential impact of this effect on daily albedo, we corrected albedo based on the theoretical relationship between irradiance for horizontal and tilted planes of incidence, assuming a constant slope angle of 6° and an aspect of 73° (northeast). For a horizontal incident plane, albedo can be calculated as the ratio of reflected to incoming radiation:

$$albedo = \frac{SW_{ref}}{SW_{in}}$$

In the case of a tilted reflecting surface, the measured parameter  $SW_{ref}$  represents the incoming radiation on the tilted plane as reflected into the downward facing sensor, such that:

$$SW_{ref} = SW_{tilted} * albedo$$

Where  $SW_{tilted}$  is a function of - mainly -  $SW_{in}$ , the solar position on a given day, and the slope and aspect of the surface. To assess the magnitude of the error introduced by the tilt of the surface, we computed a corrected albedo (albedo\_cor) as the ratio of  $SW_{ref}$  to  $SW_{tilted}$ . In addition to the solar position, calculating  $SW_{tilted}$  requires estimates of the diffuse horizontal irradiance (DHI) and direct normal irradiance (DNI) components of global hemispherical irradiance (GHI) as measured by the upward facing sensor. We applied Boland's method (Boland et al., 2013) as implemented in the python package pvlib (Anderson et al., 2023; Jensen et al., 2023) to decompose measured GHI ( $SW_{in}$ ) into DNI and DHI.  $SW_{tilted}$  was then

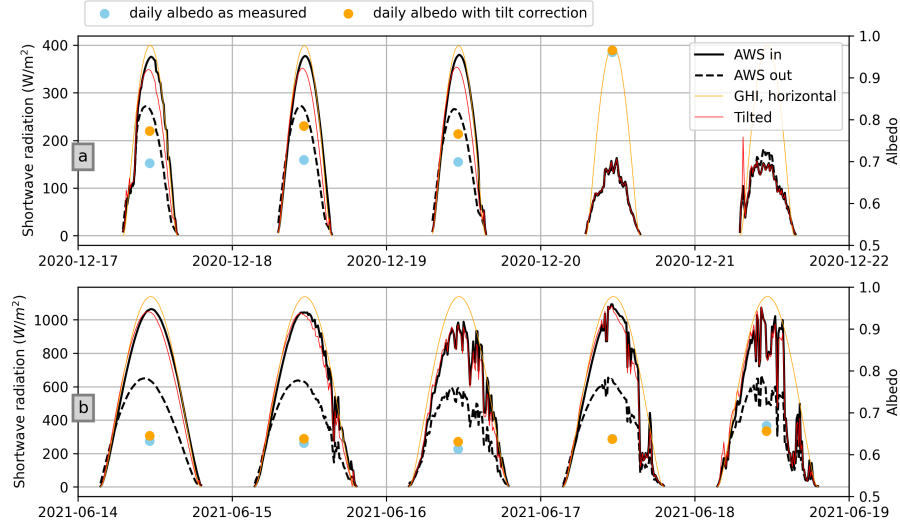


**Figure S1.** Diurnal cycle of incoming and reflected radiation for example time periods in winter (a) and summer (b). Black lines mark the measured shortwave incoming (AWS in) and reflected radiation (AWS out, dashed). Global hemispherical irradiance (GHI) for a horizontal surface was computed based on the sun angle and location. The red line indicates the irradiance for a plane with a slope angle of  $6^\circ$  and an aspect of  $73^\circ$  computed from the measured incoming radiation. Daily albedo as measured ( $SW_{ref}/SW_{in}$ ) is shown in blue, the corrected albedo estimate in orange ( $SW_{ref}/SW_{tilted}$ ).

computed as the sum of direct beam irradiance and diffuse irradiance from the sky, both over the tilted plane of incidence, assuming an isotropic sky model also as implemented in the pvlib package.

The difference between raw and corrected values has a seasonal cycle determined by the sun angle and reaches highest values on cloud free days in the winter months. In summer, corrections are typically below +0.02 on cloud free days. On days with cloud cover, the correction values are negligible due to the increased contribution of diffuse radiation. For the entire data set, the median correction value is 0.04 in January, and 0.001 and 0.002 in July and August, respectively (Fig. S2). Hence, we consider the impact small compared to the assumed measurement uncertainty of the sensor. We note that other kinds of analyses may require more sophisticated corrections for the tilt, especially if addressing sub-daily resolution albedo during the winter months (Abermann et al., 2014; Weiser et al., 2016).

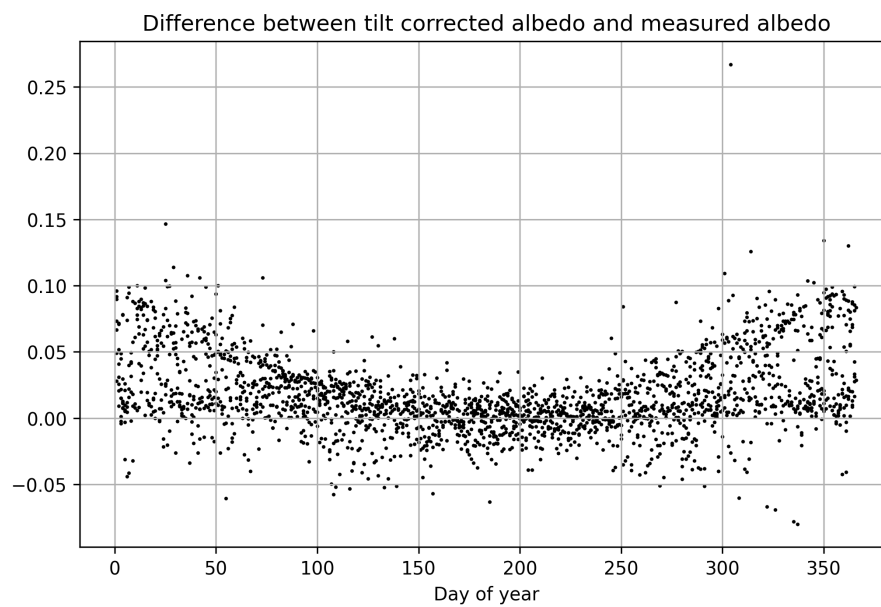


**Figure S2.** Difference between the daily albedo estimate corrected for the tilt of the surface and the uncorrected values plotted against the day of the year. Values are shown for the entire data set.

The data records from the ultrasonic ranger (SR50) contain considerable noise. The exact cause of this problem has not been determined but is likely related either to a problem with the unheated sensor (the problem persisted to a lesser degree after the sensor was replaced), to spurious signals from a guy wire, the control box, rime or blowing snow, or a combination of these factors.

35 We used the SR50 data to determine surface height change and estimate snowfall for the example period used for model evaluation shown in Fig. S8. Fig. S3 shows the uncorrected data compared to the smoothed surface height. Data were smoothed as follows:

- Manual removal of outlier values with unrealistic amount of surface change or unrealistic surface values
- Removal of surface values where the difference between the value and the 48 hour rolling mean is greater than 15 cm.
- 40 – Extraction of the lower envelope of the remaining data and linear interpolation to fill resulting gaps.
- Computation of the 24 h rolling mean to smooth the resulting surface height time series
- Snowfall was calculated as the difference between consecutive hourly surface height values if the change is positive and set to zero if it is negative.

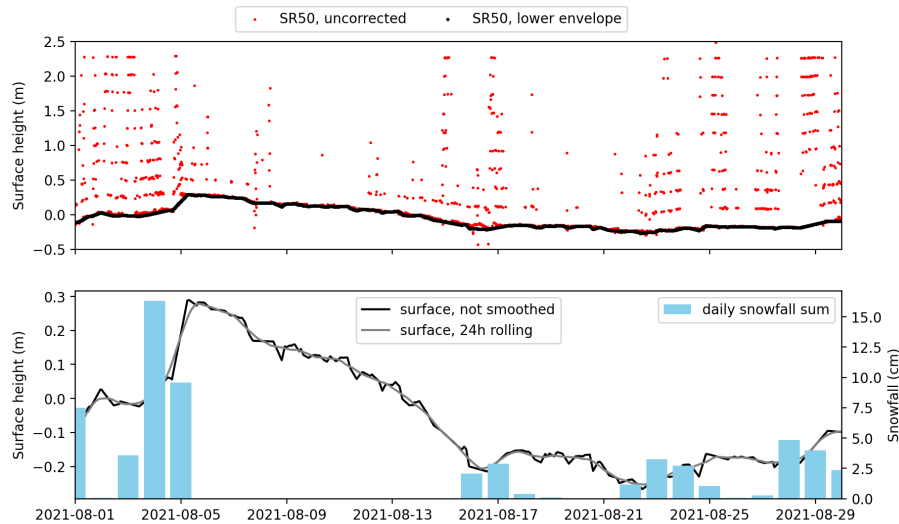


**Figure S3.** Upper panel: SR50 records without correction (red) and after smoothing and extraction of the lower envelope (black). Values are shown in relation to the height of the sensor above the ice surface at the time of installation (surface height = 0). Negative values indicate ice ablation since the time of installation.

### 3 Additional supplementary material



**Figure S4.** Automatic camera images taken on or close to the date of the seasonal minimum albedo recorded by the AWS. Red ellipses indicate the AWS position. Photos were taken on August 21, 2018; August 24, 2019; September 20, 2020; August 15, 2021; August 11, 2022; August 25, 2023; September 8, 2024.

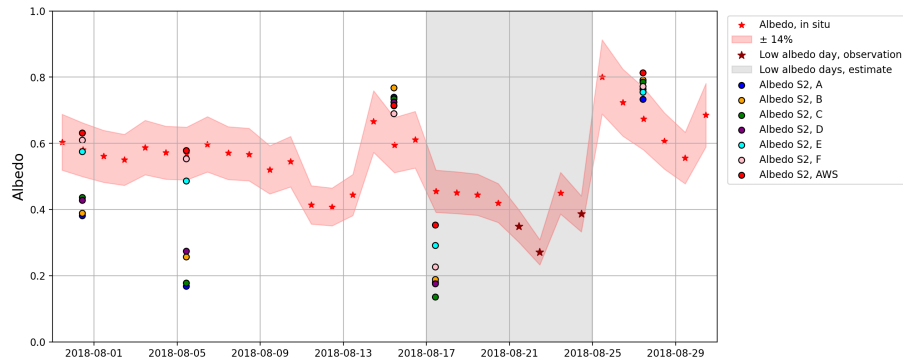


**Figure S5.** Daily albedo as observed at the AWS with  $\pm 14\%$  uncertainty shown as red shading. S2-derived albedo at the stake locations and AWS shown as circular markers. The grey shading indicates the days counted as "estimated low albedo days" at the AWS.

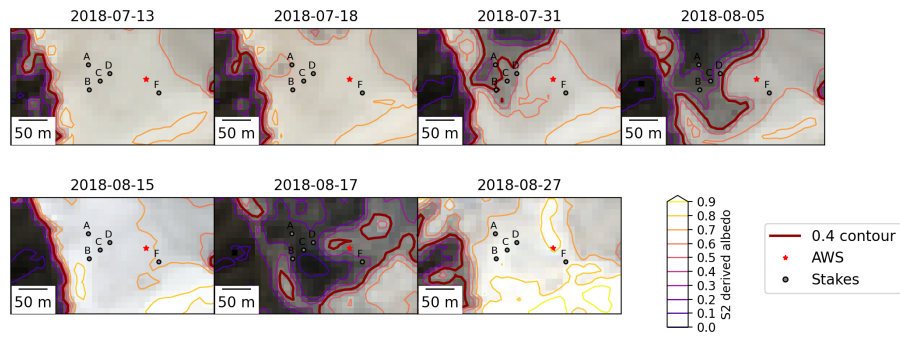


**Figure S6.** RGB composites of the WSS summit region in summer 2018. The contour lines indicate S2-derived albedo. The 0.4 contour ("low albedo" threshold) is highlighted as a thicker line.

**Table S1.** Modelled daily SMB averaged over 15 day time periods of average July-September conditions and different albedo values.

	SMB for albedo 0.1[mm w.e.]	SMB for albedo 0.20 [mm w.e.]	SMB for albedo 0.40 [mm w.e.]	SMB for albedo 0.60 [mm w.e.]
Jul 1-Jul 15	-44	-39	-28	-17
Jul 16-Jul 30	-43	-38	-29	-19
Jul 31-Aug 14	-40	-36	-26	-17
Aug 15-Aug 29	-36	-32	-23	-15
Aug 30-Sep 13	-30	-26	-18	-11
Sep 14-Sep 29	-19	-15	-9	-4



**Figure S7.** Photos of stakes A, C, and D and the AWS taken during stake readings on August 29, 2018.

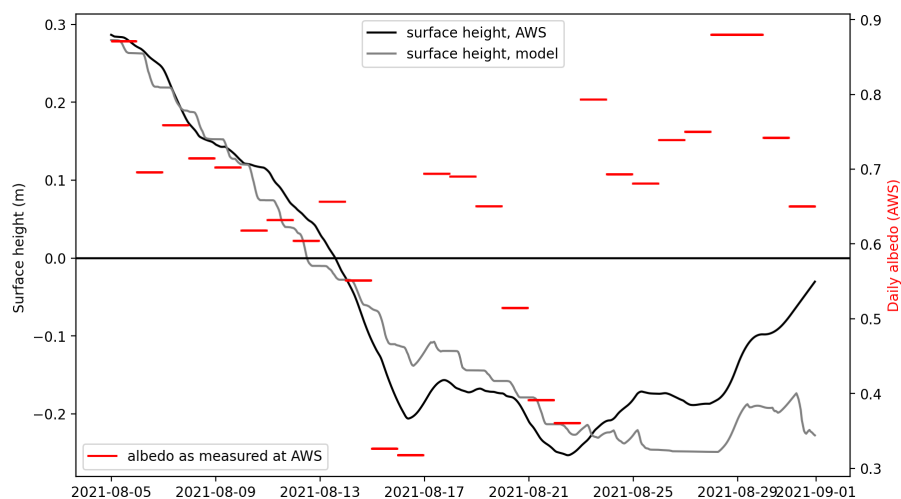


**Figure S8.** Surface height at the AWS in July 2021 as measured with the SR50 (smoothed as described above) and as COSIPY model output; daily albedo (right axis) was used as an input parameter for the model. Surface height is shown in reference to the ice surface at the time of installation of the SR50.

## 45 **References**

- Abermann, J., Kinnard, C., and MacDONELL, S.: Albedo variations and the impact of clouds on glaciers in the Chilean semi-arid Andes, *Journal of Glaciology*, 60, 183–191, 2014.
- Anderson, K. S., Hansen, C. W., Holmgren, W. F., Jensen, A. R., Mikofski, M. A., Driesse, A., et al.: pvlib python: 2023 project update, *Journal of Open Source Software*, 8, 5994, 2023.
- 50 Boland, J., Huang, J., and Ridley, B.: Decomposing global solar radiation into its direct and diffuse components, *Renewable and Sustainable Energy Reviews*, 28, 749–756, 2013.
- Jensen, A. R., Anderson, K. S., Holmgren, W. F., Mikofski, M. A., Hansen, C. W., Boeman, L. J., and Loonen, R.: pvlib iotools—Open-source Python functions for seamless access to solar irradiance data, *Solar Energy*, 266, 112 092, 2023.
- Weiser, U., Olefs, M., Schöner, W., Weyss, G., and Hynek, B.: Correction of broadband snow albedo measurements affected by unknown  
55 slope and sensor tilts, *The Cryosphere*, 10, 775–790, 2016.